Lifecycle Operational Reliability Assessment of Water Distribution Networks Based on Artificial Neural Network

Wei Liu
Associate Professor, Dept. of Structural Engineering, Tongji University, Shanghai, China

Associate Professor, State Key Laboratory of Disaster Reduction in Civil Engineering, Tongji University, Shanghai, China

Zhiyin Xie
Graduate Student, Dept. of Structural Engineering, Tongji University, Shanghai, China

ABSTRACT: Failures in water distribution networks (WDNs) can not only lead to water and financial losses, but also affect the normal operation of the city. To assess the reliability of WDNs, this paper first uses an artificial neural network to predict pipe failure probability and input features' impact on pipe failure is calculated. In addition, the failure simulation models consider leak and burst scenarios. Then, Monte Carlo simulation is employed to calculate nodal reliabilities of a real-world WDN and factors influencing reliability are analyzed. Results show that physical and socioeconomic factors can affect pipe failure probability. Moreover, operation time, pipe roughness, the distance from source to the node and the loop configuration can all have impact on the reliability.

A reliable water distribution network (WDN) is the foundation of industrial activities and residential life (Li and Liu 2020). However, due to various unexpected events, including pipe aging, overuse and disrepair, WDNs are prone to failures such as leaks and bursts (Liu et al. 2020). These failures can not only lead to resources and financial losses, but also affect normal operation of the city. Therefore, it is of great significance to assess the reliability of WDNs in order to determine vulnerable components of WDNs and facilitate management practice for decision-makers. The reliability of a WDN can be defined as the probability of satisfying consumers' demands under normal and failure circumstances of pipes throughout a lifecycle (Shinstine et al. 2002).

To estimate the pipe failure probability, there are three types of methods in general, namely, physical models (Rajani and Kleiner 2001), statistical models(Yamijala et al. 2009), and machine learning (ML) models (Fan et al. 2022). Physical models are of clear physical sense (Rajani and Kleiner 2001) but require intensive computation efforts (Fan et al. 2022). Statistical models are cost-effective (Yamijala et al. 2009). However, few physical factors, such as pipe age and length, are considered for simplification (Liu et al. 2020). Recently, with the advancement of artificial intelligence technology and the increasing amount of WDNs data available, data-driven ML models, including but not limited to artificial neural networks (ANNs) (Fan et al. 2022), tree-based models (Liu et al. 2022), and support vector classifications (Robles-Velasco et al. 2020), have been widely used to predict pipe failure. Compared to the other two models, ML models not only achieve better prediction accuracy cost-effectively from an objective perspective, but also can reveal the complex relationship between factors and failure probability (Almheiri et al. 2021).

Methods of computing the reliability of WNDs include analytic, surrogate-measure, moment and simulation approaches (Gheisi et al. 2016). Analytic approach assumes a node is reliable if it is connected to a source (Wagner et al. 1988). However, this condition is only a necessary but not sufficient condition (Ostfeld 2004). Surrogate-measure approach alleviates

computation labors but is experience-based methods with highly subjectivity (Gheisi et al. 2016) and disregards the randomness in WDNs to a certain degree (Liu et al. 2020). Moment approach, such as first-order and second-moment (FOSM) method, can only obtain the moments of target responses of a system and leads to serious reduction in accuracy (Liu and Li 2010). Apparently, the complexity and nonlinearity of WDNs pose difficulties in quantifying reliability within an acceptable error. Simulation approach measures the probability that a partly or completely failed WDN can meet consumers' demands through simulation techniques, including Monte Carlo simulation (MCS) (Ostfeld 2004). Compared to other methods, MCS can assess reliability accurately and take randomness in WDNs into consideration.

In this paper, since ANN can achieve better accuracy than other ML algorithms, an ANN is used to predict failure probability of pipes, which are major components of WDNs. However, ANN is too complexed to be as explainable as others. To address this issue, Shapley Additive exPlanations (SHAP) (Lundberg and Lee 2017) method is employed to calculate each feature's contribution to pipe failure. In addition, to our best knowledge, few studies on pipe failure prediction consider socioeconomic factors, which are proved to have an important impact on the pipe conditions (Fan et al. 2022). Therefore, the dataset for ANN in this study includes socioeconomic factors to improve the predictive performance. Moreover, failure simulation models are used to simulate the performance of WDNs in the case of leaks or bursts occurring to partial pipes. Then, MCS is employed to assess lifecycle operational reliability of a real-world WDN.

1. PIPE FAILURE PREDICTION MODEL

1.1. Structure of ANN

An ANN is made of an input layer, several hidden layers, and an output layer. Hidden layers serve as a sequence of operators extracting feature information in input vector $\mathbf{x}_0$. The output of the ith hidden layer $\mathbf{x}_i$ is calculated by

$$\mathbf{x}_i = f\left(BN\left(\mathbf{W}_i\mathbf{x}_{i-1} + \mathbf{b}_i\right)\right) \tag{1}$$

where $\mathbf{W}_i$ and $\mathbf{b}_i$ denote the weight matrix and bias vector of the ith hidden layer; i = 1, 2, …, L, respectively; L is the number of hidden layers; BN represents batch normalization that speeds up convergence (Ioffe and Szegedy 2015); $f(\cdot)$ is rectified linear unit (ReLU) activation function , namely, $f(\cdot) = \max(0, \cdot)$ (Goodfellow et al. 2016). Output layer uses a softmax classifier to generate the probability distribution for the predicted classes in the range [0, 1] according to

$$p\left(y = k\right) = \frac{\exp\left(\mathbf{W}_{L+1}\mathbf{x}_L\left[k\right]\right)}{\sum_{k=1}^{K}\exp\left(\mathbf{W}_{L+1}\mathbf{x}_L\left[k\right]\right)} \tag{2}$$

where K is the number of classes; $p(y = k)$ indicates the probability that a given sample $\mathbf{x}$ belongs to the kth class (k =1, 2, ⋯, K); $\mathbf{W}_{L+1}$ is the connecting weight matrix between the last hidden layer and the output layer; $\mathbf{W}_{L+1}$ $\mathbf{x}_L[k]$ represents the kth element of the resultant vector of multiplying $\mathbf{W}_{L+1}$ and $\mathbf{x}_L$. In this study, pipe failures include leak and burst. Hence the probability that a given pipe sample $\mathbf{x}$ belongs to the state of normal, leak and burst, can be expressed as p_N, p_L, and p_B, respectively. Finally, the state of pipe $\mathbf{x}$, (i.e., y) is predicted as the class corresponding to the maximal probability.

1.2. Dataset for ANN

The maintenance dataset provided by the water administration sector is used to train and test the ANN. The dataset includes physical properties and socioeconomic characteristics. Physical properties include length (LEN), material (MAT), diameter (DIA) and service age (AGE). Socioeconomic features include area of the district (AD), population density of the district (PD), housing area constructed (HAC), and gross domestic product per capita (GDPC) of the district. In addition, the supervisory variable is the failure record (FR) of each individual pipe. Only MAT is category feature and MATs include ductile cast iron pipes (DIPs), steel pipes (SPs), cast iron pipes (CIPs), polyethylene pipes (PEEPs), polyvinyl chloride pipes (PVCs), and concrete pipes (CPs).

After cleaning abnormal and missing data, there are 54,400 pipe samples available, including 6,369 leakage samples and 620 burst samples. In order to estimate the generalized predictive performance of ANN on unseen pipes, the dataset is divided into training set and test set by the ratio of 9:1 and the ratios of the three types of supervisory labels in both two sets are kept the same. The ratio of the number of normal samples, leak samples and burst samples is about 77:10:1, which exhibits the imbalanced nature. This can lead to a decline in the prediction performance for the samples with minority class (Liu et al. 2022). Therefore, to improve the prediction ability, an improved oversampling technique, namely, synthetic minority oversampling techniques (SMOTE) (Chawla et al. 2002) is adopted to balance the training set.

Note that the supervisory label FR records whether leak or burst occurred in a year, not the number of occurrences. Therefore, the output of ANN (i.e., p_L and p_B), indeed, are the probabilities that one pipe leaks or bursts at least once a year, which are represented by p_L^Y and p_B^Y, respectively. In this study, it is assumed that failures of different pipes threaten the operation reliability at the same time only if their failures occur on the same day. Hence, the daily failure probability is considered in the following assessment of reliability. Based on the assumption that the number of occurring failures obeys Poisson distribution and the failure rate at each day in one year keeps constant (Liu et al. 2020), daily failure probability p_F^D is obtained by

$$\lambda_F^D = \lambda_F^Y/365 = -\frac{1}{365L}\ln\left(1-p_F^Y\right) = -\frac{1}{365L}\ln\left(1-\left(p_L^Y+p_B^Y\right)\right) \quad (3)$$

$$p_F^D = 1-e^{-\lambda_F^D L} = 1-\left(1-p_F^D\right)^{\frac{1}{365}} = 1-\left(1-\left(p_L^D+p_B^D\right)\right)^{\frac{1}{365}} \quad (4)$$

where λ_F^Y (/km/year) and λ_F^Y (/km/day) are yearly and daily failure rate, respectively; L (km) is the pipe length. Then, the daily leak probability p_L^D and burst probability p_B^D are assumed to be proportional to p_L^Y and p_B^Y, respectively as follows:

$$p_L^D = p_F^D\frac{p_L^Y}{p_L^Y+p_B^Y},\ p_B^D = p_F^D\frac{p_B^Y}{p_L^Y+p_B^Y} \quad (5)$$

1.3. Performance of ANN

The predictive performance of ANN is evaluated by a normalized confusion matrix $\mathbf{C} = [c_{ij}]$. c_{ij}, in which $i, j \in$ {Normal, Leak, Burst}, represents the ratio between the number of class i samples predicted to be class j samples and the number of class i samples. Clearly, larger c_{ii} ($i = j$) and smaller c_{ij} ($i \neq j$) indicate better prediction capacity of ANN for it can predict more pipes' states accurately. Figure 1 shows the normalized confusion matrix of the ANN. All normal pipes, 99% of leak pipes and 86% of burst pipes are predicted correctly, while only 1.4% of leak pipes are predicted as burst pipes. Thus, ANN can identify normal and failure pipes nearly perfectly since neither leak pipes nor burst pipes are classified as normal, which is safe for design of maintenance strategy. Nevertheless, 14% of burst pipes are predicted to leak, which indicates a relatively poor ability for ANN to distinguish between leak and burst, but it is still acceptable considering the complexity and difficulty of predicting pipe failure. In general, the ANN performs well.

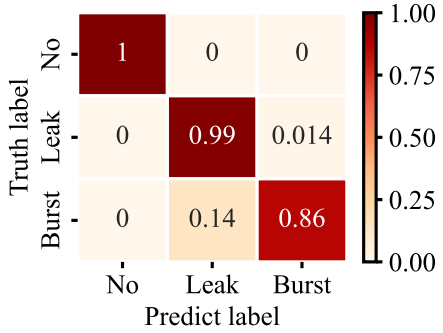

Figure 1 Normalized confusion matrix of ANN (No denotes the normal state)

In this study, SHAP (Lundberg and Lee 2017) method is employed to calculate each feature's

impact on pipe failure probability. A higher magnitude of SHAP value of a feature indicates the feature has a larger impact on the pipe failure probability. If a higher feature value corresponds to a higher SHAP value, the feature has a positive impact on the failure probability and vice versa. Figure 2 shows SHAP values of continuous variables, which is colorized for their magnitudes and top to bottom represents the highest to lowest level of feature's influence. Figure 3 shows SHAP values of MAT. For physical features, AGE and LEN both have a positive effect on failure probability, while DIA has a negative one. In terms of MAT, CIPs and PVCs have the positive SHAP values while SPs, DIPs and PEEPs have the negative ones. Regarding socioeconomic factors, PD has a positive impact on failure probability while the AD's effect on failure is negative. Additionally, GDPC does not show an evident correlation with the failure probability. HAC is ranked the last and has a positive influence on failure.

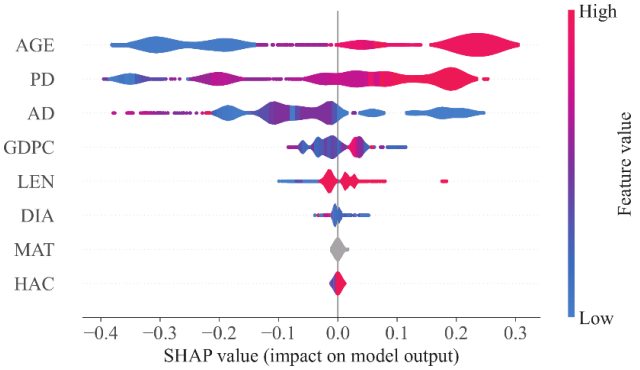

Figure 2 SHAP values plots

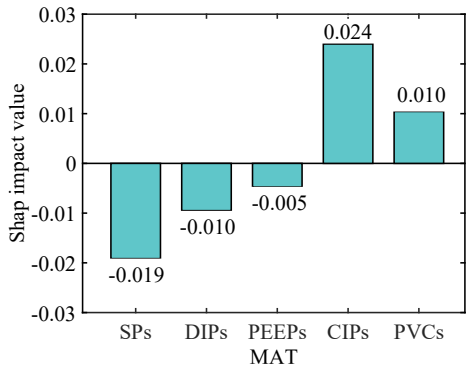

Figure 3 SHAP values of MAT

2. FAILURE SIMULATION MODELS OF WDNS

For each pipe in the WDN assessed, three intervals, i.e., $[0, p_L^D)$, $[p_L^D, p_L^D + p_B^D)$, and $[p_L^D + p_B^D, 1)$, can be obtained. For each simulation, a random number k_F is generated and the state of the pipe is determined by which interval k_F lies in. Leak and burst scenarios are simulated in two different ways as follows.

2.1. Leak

A general hydraulic equilibrium equation considering the transportation ability deterioration resulted from leaks is expressed as (Liu et al. 2020)

$$\mathbf{A}\mathbf{Q}_P + \mathbf{Q}_N + \mathbf{Q}_L = \mathbf{0} \tag{6}$$

where $\mathbf{A}=[a_{ij}]$ is the matrix indicating the connection relationship between nodes and pipes, which equals to 1 if water in pipe j flows out of node i; −1 if water in pipe j flows into node i and 0 if pipe j is not connected to node i; $\mathbf{Q}_P$ represents the pipe flow vector; $\mathbf{Q}_N$ denotes the nodal flow vector; and $\mathbf{Q}_L$ indicates the leak flow vector. For a given pipe, the leak flow is calculated by (Liu et al. 2020)

$$q_L = 0.6\varphi A_L \sqrt{2gH_L} \tag{7}$$

where q_L indicates the leak flow; φ denotes the leak coefficient; g is the gravity acceleration; H_L represents the head of the leak point; and A_L is the leak area. Herein, A_L is considered to be a random variable that satisfies the uniform distribution in [0.1%S, 20%S] in which S is the pipe section area. $\mathbf{Q}_P$ is calculated by

$$q_P = 0.278 C_{HW} D^{2.63} \Delta H^{0.54} L^{-0.54} \tag{8}$$

where q_P denotes the pipe flow; D is the pipe diameter; ΔH represents the head difference between two leak nodes; L is the pipe length; and C_{HW} indicates the Hazen-Williams coefficient relevant to roughness and is calculated by (Sharp and Walski 1988)

$$C_{HW} = 18.0 - 37.2 \log \frac{e_0 + aT}{D} \tag{9}$$

where T (year) is the operation time and other variables can refer to (Liu et al. 2020).

2.2. Burst

A burst occurring to a pipe will lead to serious consequences such as considerable waste of water and head loss if the burst pipe is not isolated by closing relevant valves timely. Thus, valves in adjacent pipes are supposed to be closed. In this study, an algorithm based on depth-first search (DFS) (Liu et al. 2020) is used to isolate burst pipes with least pipes impacted. After closing valves in influenced pipes and isolating all burst pipes, the topology of a WDN can change. Flow analysis (i.e., solving Eq. (6)) should be performed on the new WDN to calculate nodal heads.

3. DEFINITION OF RELIABILITY

The lifecycle operational reliability of a WDN is defined as the probability of satisfying consumers' demands under normal and failure circumstances of pipes throughout a lifecycle. For a consumer node, if the nodal head exceeds the demand head, the node is assumed to be able to offer consumers sufficient water and thus we consider the node reliable and vice versa (Liu et al. 2020). Therefore, the reliability can be calculated by MCS as follows:

$$R_i = \Pr\left\{H_i \geq H_i^0\right\} = \frac{1}{N}\sum_{k=1}^{N} I\left(H_{ik} \geq H_i^0\right) \quad (10)$$

where R_i is the reliability of node i; H_{ik} denotes the head of node i at the kth simulation; H_i^0 indicates the demand head of node i, which takes 20 m in this paper; N is the number of simulations, which takes 5000 in this paper; $I(\cdot)$ is indicator function, and $I(Q) = 1$ only if event Q holds true, otherwise $I(Q) = 0$.

4. CASE STUDY

4.1. Introduction to case WDN assessed

The lifecycle operational reliability of a real WDN in Mianzhu City, China is assessed in this paper. The total length of the main pipes is about 44 km. The simplified topology configuration includes 82 nodes, 107 pipes and 92 valves as shown in Figure 5.

4.2. Results and discussion

Nodal reliabilities in the 5th, 20th, 35th, 50th year are shown in Figure 4. Computation costs 2.5h totally. As can be seen, the reliability of each node in the 5th year almost equals to 1, which means the WDN can provide consumers with sufficient water. The reliability in the 20th year decreases, but the decreasing magnitude is small, indicating that the WDN can basically meet consumers' requirements with the minimal reliability of 0.993. By the 35th year, the decline in reliability is greater and the difference between nodes becomes relatively apparent. Additionally, the reliability decreases more in the 50th year and the decreasing magnitude the differ evidently between nodes. For example, the decreasing magnitudes of nodes 71 ~ 76 are evidently larger than those of other nodes. To sum up, the reliability decreases with time and increasing magnitude. This deterioration with time can result from three main aspects: (1) the growth of failure probability with time since AGE has the largest positive impact; (2) the increase of PD and HAC by year; and (3) the increase of pipe roughness that further reduces the nodal heads.

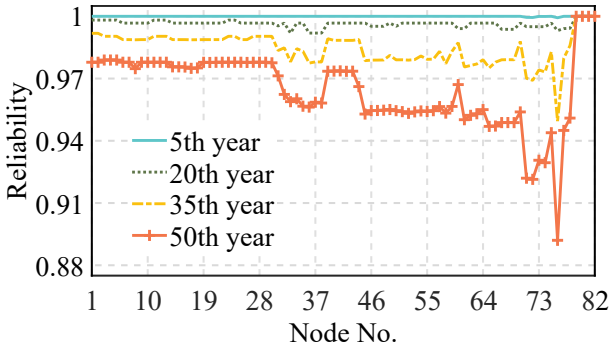

Figure 4 Nodal reliabilities in the 5th, 20th, 35th, 50th year

Figure 5 shows the variance of nodal reliabilities in the 50th year with respect of space, in which nodes are colored with their reliability values. In addition, Figure 6 describes the relationship between the nodal reliability in the 50th year and the length of the shortest path that connects the node and its nearest source. The cor-

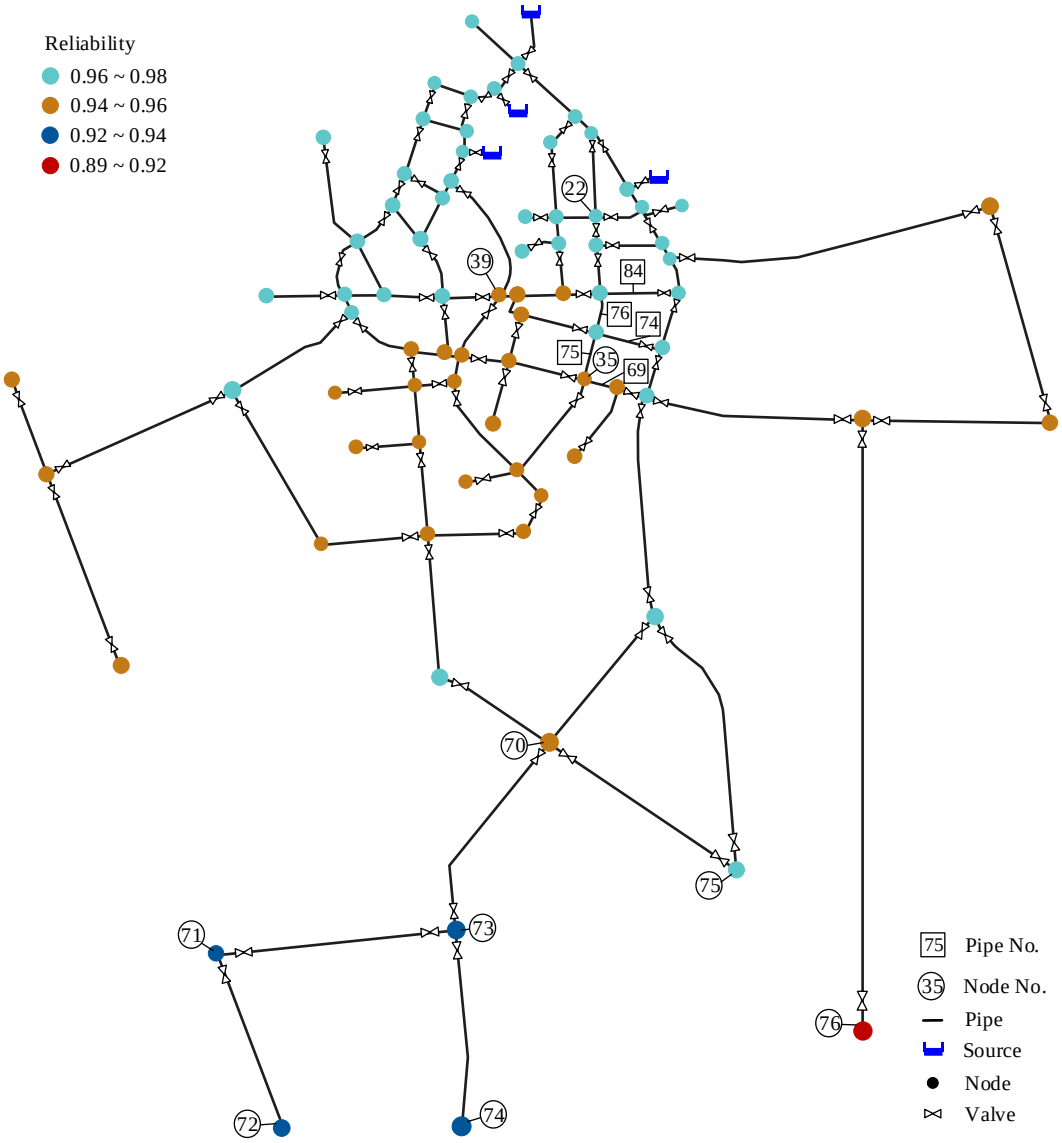

Figure 5 The variance of nodal reliabilities in the 50th year with respect of space

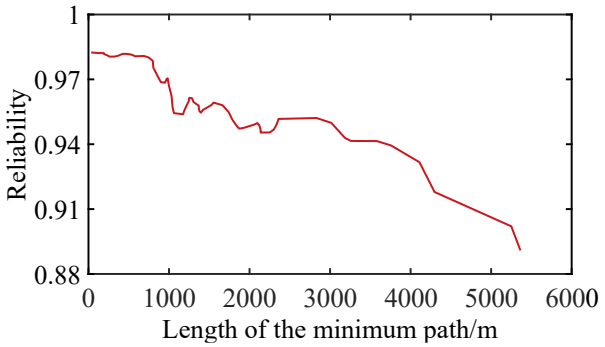

Figure 6 The relationship between nodal reliability in the 50th year and the length of minimum path (the correlation coefficient R^2 is −0.869)

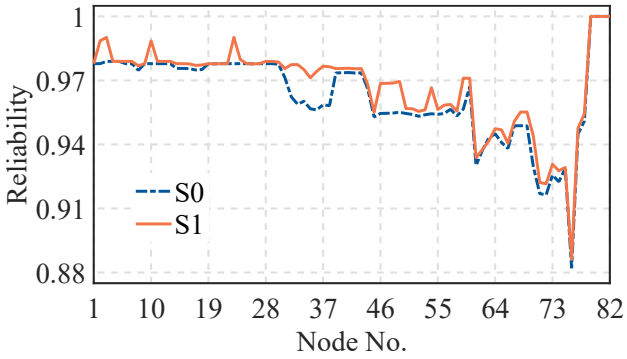

Figure 7 Nodal reliabilities of the WDN in the 50th year in case of S0 and S1

relation coefficient R^2 is −0.869. The shortest path is searched by a modified Dijkstra Algorithm (Liu and Wu 2009). Some conclusions can be drawn based on observations. First, the reliability decreases with the distance from the source due to more serious on-way head loss and higher failure probability occurring to upstream pipes on the path. Second, nodal reliability differs per the pipe loop configuration. In general, a well-looped configuration ensures that a node, such as node 22 and 39, can be sufficiently supplied by multiple pipes, especially when one of adjacent pipes is isolated owing to burst. This thus enhances the reliability. For nodes in the tree-like areas such as node 76, once a leak or burst occurs to the pipe connected to the node, the node cannot receive water from other pipes.

The number of valves has a serious impact on the reliability as well. To demonstrate the influence of the valve condition, we simulate one case for comparison, namely, S1: set the number of valves in each pipe to two. Let case S0 correspond to the valve configuration showed in Figure 5. The nodal reliabilities in the 50th year in two cases are depicted in Figure 7. As can be seen, with two valves located in each pipe, the nodal reliabilities increase. For example, in case of S0, node 35 cannot be supplied when a burst occurs to one of pipes 69, 74, 75, 76 and 84. However, in case of S1, node 35 is isolated only if its four adjacent pipes burst at the same time, which is almost impossible to occur during daily operation. In addition, in case of S1, the reliabilities of partial nodes, such as node 75, are almost the same as those in case of S0. One possible reason is that these nodes are connected to pipes with two valves in case of S0 and hence there is no difference between S1 and S0 for these nodes.

5. CONCLUSIONS

In this paper, an ANN is used to predict pipe failure probability and the SHAP method is employed to compute features' impact on failure. The failure simulation model considers leaks and bursts. Then, MCS is employed to calculate nodal reliabilities of a real-world WDN. The results show that (1) service age, pipe length, population density and housing area constructed have a positive effect on failure while area of district and pipe diameter have a negative one; (2) nodal reliability decreases as failure probability and pipe roughness increasing with time; (3) the distance from source to the node and the loop configuration both have influence on nodal reliability; (4) the more pipes with two valves in the WDN, the less nodes influenced by a burst occurring to a distant pipe.

Note that although MCS can give the precise results, computation costs a lot of time especially for large-scale WDNs. Future work can focus on cost-effective methods such as probability density evolution method to compute reliability to alleviate computation costs.

6. REFERENCES

Almheiri, Z., M. Meguid, and T. Zayed. 2021. "Journal of Water Resources Planning and Management." *Water Res.* 205 (Oct).

Chawla, N. V., K. W. Bowyer, L. O. Hall, and W. P. Kegelmeyer. 2002. "SMOTE: Synthetic minority over-sampling technique." *J. Artif. Intell. Res.* 16 (Jan): 321-357.

Fan, X. D., X. W. Wang, X. J. Zhang, and P. E. F. A. X. Yu. 2022. "Machine learning based water pipe failure prediction: The effects of engineering, geology, climate and socio-economic factors." *Reliab. Eng. Syst. Safe* 219 (Mar).

Gheisi, A., M. Forsyth, and G. Naser. 2016. "Water Distribution Systems Reliability: A Review of Research Literature." *J. Water Res. Plan. Man.* 142 (11).

Goodfellow, I., Y. Bengio, and A. Courville. 2016. *Deep Learning*. Cambridge, MA: MIT Press.

Ioffe, S., and C. Szegedy. 2015. "Batch Normalization: Accelerating Deep Network Training by Reducing Internal Covariate Shift." In *Proc., 32nd Int. Conf. Mach. Learn.*, 448-456. San Diego, CA: JMLR.

Li, J., and W. Liu. 2020. *Lifeline Engineering Systems: Network Reliability Analysis and Aseismic Design*. Singapore: Springer Nature.

Liu, C., and J. Wu. 2009. "Scalable Routing in Cyclic Mobile Networks." *IEEE T. Parall Distr.* 20 (9): 1325-1338.

Liu, W., and J. Li. 2010. "Seismic Functional Reliability Analysis of Urban Water Distribution

Network." In *Proc., 11th Int. Symp. Struct. Eng.*, 1828-1832. Beijing: Science Press Beijing.

Liu, W., B. H. Wang, and Z. Y. Song. 2022. "Failure Prediction of Municipal Water Pipes Using Machine Learning Algorithms." *Water Resour. Manag.* 36 (4): 1271-1285.

Liu, W., Z. Y. Song, Z. Q. Wan, and J. Li. 2020. "Lifecycle operational reliability assessment of water distribution networks based on the probability density evolution method." *Probabilist. Eng. Mech.* 59 (Jan).

Lundberg, S. M., and S. I. Lee. 2017. "A Unified Approach to Interpreting Model Predictions." In *Proc., 2017 Proc. Adv. Neural Inf. Process. Syst.*, 4765-4774. Red Hook, NY: Curran Associates Inc.

Ostfeld, A. 2004. "Reliability analysis of water distribution systems." *J. Hydroinform.* 6 (4): 281-294.

Rajani, B., and Y. Kleiner. 2001. "Comprehensive review of structural deterioration of water mains: physically based models." *Urban Water* 3 (3): 151-164.

Robles-Velasco, A., P. Cortes, J. Munuzuri, and L. Onieva. 2020. "Prediction of pipe failures in water supply networks using logistic regression and support vector classification." *Reliab. Eng. Syst. Safe* 196 (Apr).

Sharp, W. W., and T. M. Walski. 1988. "Predicting Internal Roughness in Water Mains." *J. Am. Water Works Ass.* 80 (11): 34-40.

Shinstine, D. S., I. Ahmed, and K. E. Lansey. 2002. "Reliability/availability analysis of municipal water distribution networks: Case studies." *J. Water Res. Plan. Man.* 128 (2): 140-151.

Wagner, J. M., U. Shamir, and D. H. Marks. 1988. "Water Distribution Reliability - Analytical Methods." *J. Water Res. Plan. Man.* 114 (3): 253-275.

Yamijala, S., S. D. Guikema, and K. Brumbelow. 2009. "Statistical models for the analysis of water distribution system pipe break data." *Reliab. Eng. Syst. Safe* 94 (2): 282-293.